Dicle University
Journal of Engineering
https://dergipark.org.tr/tr/pub/dumf
duje.dicle.edu.tr

Research Article

Numerical Analysis of Dual Slot Pulsating Nanofluid Impinging Jets

Ali TAŞKIRAN[1], Celal KISTAK[2], Sinan KAPAN[3], Nevin ÇELİK[4*], İhsan DAĞTEKİN[5]

[1] Şırnak University, Mechanical Engineering Department, taskiranalii@gmail.com, Orcid No: 0000-0001-6810-7291
[2] Fırat University, Mechanical Engineering Department, ckistak@firat.edu.tr, Orcid No: 0000-0003-4621-5405
[3] Fırat University, Mechanical Engineering Department, skapan@firat.edu.tr, Orcid No: 0000-0001-5690-1041
[4] Fırat University, Mechanical Engineering Department, nevincelik23@gmail.com, Orcid No: 0000-0003-2456-5316
[5] Fırat University, Mechanical Engineering Department, idagtekin@firat.edu.tr, Orcid No: 0000-0003-0128-7149

ARTICLE INFO

Article history:

Received 16 October 2024
Received in revised form 25 November 2024
Accepted 29 November 2024
Available online 23 December 2024

Keywords:

Nanofluids, Impinging jets, Pulsating, Numerical simulations, ANSYS

Doi: 10.24012/dumf.1567752

* Corresponding author

ABSTRACT

Jet impingement is a well-established technique extensively employed in engineering applications, particularly for the thermal management of high-temperature systems such as aircraft engines and electronic devices. This study utilizes numerical analysis, conducted through the ANSYS software platform, to investigate the flow dynamics of dual impinging pulsating nanofluid jets. The research aims to evaluate the combined effects of key parameters, including jet geometry, pulsation frequency, amplitude, nanoparticle volume concentration, and Reynolds numbers, on the efficiency of heat transfer. The impact of aluminum oxide (Al_2O_3) nanofluids with varying concentrations (1%, 2%, 4%, and 5%) on thermal performance is assessed. The findings of the study demonstrate that the pulsating jets generate bidirectional swirling flows and reverse vortices upon impact with the surface, resulting in notable enhancements in local heat transfer rates. These vortices expand and form wall jets, which contribute to an increase in the heat transfer coefficients and Nusselt numbers. The simulations demonstrate that higher pulsation frequencies (30 Hz) result in a 10% increase in heat transfer efficiency compared to lower frequencies (10 Hz). This is attributed to enhanced flow dynamics and improved heat distribution. Moreover, the incorporation of nanoparticles markedly enhances heat transfer efficiency. The Nusselt numbers were observed to increase by 18% when the concentration of nanoparticles reached 5%, in comparison to plain water. Additionally, the study underscores the significance of jet spacing, wherein an optimal separation distance of 100 mm between the dual jets was identified as a means of maximizing heat transfer by fostering effective vortex interactions. Higher Reynolds numbers contribute to the formation of thinner thermal boundary layers, thereby facilitating increased heat transfer rates, particularly at the stagnation points where the flow impinges directly on the surface. Overall, the study demonstrates that substantial enhancements in heat transfer can be achieved by optimizing key parameters such as pulsating frequency, amplitude, nanoparticle volume concentration, and jet distances.

Introduction

Jet impingement is a prominent flow configuration with a wide range of applications across various disciplines of engineering and science. It is a technique that is commonly employed in numerous industries, including those focused on heating, cooling, drying, cutting, and cleaning. The distinctive attributes of this flow pattern have prompted considerable interest, giving rise to extensive research endeavors through both experimental and numerical investigations [1]–[6]. One of the most significant applications of impinging jets is in the cooling of high-temperature systems, such as aircraft engines and electronic devices, where efficient heat dissipation is essential for both optimal performance and safety. In addition to their utility in cooling applications, impinging air jets are indispensable in industrial drying processes across a range of sectors, including textiles, glass, and food production. In these contexts, they facilitate operational efficiency and product quality. Furthermore, this flow pattern is extensively employed in metal processing and cutting operations, where the high-speed jet impact facilitates enhanced precision and productivity.

In conclusion, the field of jet impingement remains a significant area of research interest due to its extensive applicability and its potential to optimize a multitude of industrial processes.

Impinging jets, particularly air jets, find their most widespread application in the fields of heating and cooling. In modern technological systems, these jet flows are employed to cool devices and systems that produce substantial heat or operate at high temperatures. The configuration of these flows enables efficient heat and mass transfer at the impingement region, ensuring effective cooling of the target surface. One of the notable advantages of impinging jets is their ability to achieve high local heat transfer coefficients, making them highly effective for thermal management applications.

The impingement of the fluid on the target surface effectively reduces the thickness of the thermal boundary layer at the impinging zone, thereby enhancing heat transfer and significantly increasing the rate of both heat and mass transfer on the target surface [7].

Furthermore, the utilisation of impinging jets enables the achievement of elevated heat transfer rates with a reduced quantity of fluid, which in turn optimises energy efficiency and reduces operational costs.

Research focused on improving the efficiency of impinging jets has shown that various factors, such as jet fluid properties, jet geometry, configuration (single or multiple jets), surface roughness of the target surface, and the presence or absence of jet pulsation, can significantly affect the jet impingement process [8]–[10]. While these factors have predominantly been examined individually in the literature, studies addressing the combined effects of multiple parameters remain relatively limited. This study aims to comprehensively analyze the simultaneous effects of multiple critical parameters that are known to significantly influence the impingement phenomenon during a jet impingement event.

Asem and Mishra [11] performed a numerical study to analyze the heat transfer characteristics of a high-speed air jet impinging on a flat plate under a constant heat flux boundary condition. The findings revealed a direct correlation between the Reynolds number of the jet and the acceleration of the heat transfer rate. Furthermore, the researchers identified an optimal jet-to-plate distance, which is critical for maximizing heat transfer efficiency under controlled experimental conditions. San and Chen [12] investigated the Nusselt number distribution for five circular air jets impinging vertically on a flat surface. Study revealed that the range of maximum Nusselt numbers increased linearly as the spacing between the jets in the array was widened. Chougule et al. [13] conducted both experimental and numerical investigations into the fluid flow and heat transfer characteristics of multiple air jets impinging on a flat plate. The effects of Reynolds number, target spacing-to-jet diameter ratio, and the average Nusselt number on the target plate were examined using the SST κ–ω turbulence model. The study concluded that the spacing between the air jets is a critical factor influencing the performance of multiple jet impingement systems. Similarly, Calıskan et al. [14] conducted both experimental and numerical studies to evaluate the effects of jet geometry on flow and heat transfer characteristics for elliptical and rectangular jet arrays. A thermal infrared camera was used to obtain detailed heat transfer measurements on smooth surfaces for both jet geometries. The velocity distributions obtained from numerical simulations allowed researchers to analyze the impact of jet geometry on flow dynamics and heat transfer characteristics. Additionally, numerical analyses were performed to investigate the time-dependent heat transfer performance of small-scale impinging jets at various Reynolds numbers and dimensionless *H/D* ratios, particularly in cases where significant temperature differences existed between the jet and the target plate.

Pakhomov et al. [15] conducted a numerical investigation to analyze the flow structure and heat transfer characteristics of a turbulent air jet impinging on a surface. The objective of their research was to investigate the impact of pulse frequency, jet-to-plate distance, and Reynolds number on the efficiency of heat transfer.

The findings indicated that heat transfer increases as the jet is positioned farther from the pipe edge and target surface. However, this effect diminishes when the distance becomes excessively large. Furthermore, it was determined that an elevated Reynolds number has a detrimental effect on the efficiency of heat transfer.

In the low-frequency range of the pulsed impinging jet, a reduction in heat transfer efficiency was observed in comparison to a steady-state impinging jet. Mladin and Zumbrunnen [16] conducted experimental research to investigate the influence of flow oscillations on the complex local heat transfer characteristics of a flat air jet. Their study meticulously synchronized heat transfer measurements with thermal anemometry flow data, thereby enabling a detailed analysis of the intricate link between periodic flow structures and fluctuations and heat transfer dynamics. Sailor et al. [17] in their investigation, examined the effects of a pulsating air jet impinging on a heated surface by varying jet parameters such as jet-to-plate distance, Reynolds number, and pulsation frequency. Results demonstrated that the flow cycles generated by the pulsating impinging jet led to over a 50% increase in heat transfer. Similarly, Zulkifli et al. [18] studied the impact of pulsation frequencies from a heated circular air jet on local heat transfer. By analyzing the velocity profiles of both steady-state and pulsating air jets at frequencies of 10 and 20 Hz, they concluded that the Nusselt number for the pulsating jet was higher than that of the steady jet, as the elevated frequencies enhanced heat transfer efficiency.

Demircan and Türkoğlu [7] investigated the impact of diverse parameters, including the distance ratio between plates, jet velocity, pulsation amplitude, and frequency, on a pulsating air jet discharged from a rectangular nozzle situated on the upper plate and directed onto a heated lower plate within a system comprising two horizontally parallel infinite plates. The findings indicated that as the distance between the plates increased, the stagnation Nusselt number decreased; however, this decrease was minimal when the height-to-width (*H/W*) ratio exceeded 2. At lower *H/W* ratio values, the stagnation Nusselt number closely approximated that of a steady jet, while the Nusselt number for the pulsating jet exceeded that of the steady jet. Additionally, Zao and Cheng [19] conducted both experimental and numerical studies to investigate laminar pulsating forced convection in a long tube subjected to uniform heat flux and counterflow air conditions.

In their study, Demircan and Türkoğlu [20] performed a numerical analysis of the flow and heat transfer characteristics of pulsating air jets impinging on a flat surface, wherein the jet velocity demonstrated a sinusoidal variation over time. The numerical simulations examined the effects of Reynolds number, amplitude, and jet pulsation frequency on flow and heat transfer. The results indicated that the Nusselt number exhibited a moderate increase when the jet was pulsating in comparison to a steady-state jet. The principal objective of this study is to conduct a comprehensive investigation into the influence of diverse factors on the performance and characteristics of double impinging jets. Previous research has predominantly focused on analyzing these factors in the context of single jet flows. In contrast, this study seeks to investigate them collectively to provide a comprehensive understanding of their interactions and

combined effects on heat transfer and flow dynamics In particular, this study focuses on key parameters, including jet geometry, flow characteristics, pulsating frequency and amplitude, nanoparticle volume concentrations, and Reynolds numbers, with the aim of evaluating their impact on heat transfer efficiency and the overall performance of double impinging jets.

Chaugule et al. [21] experimentally investigated the effects of applying pulsation to the impinging surface of a free turbulent jet on fluid dynamics and heat transfer. The study was conducted for two different Reynolds numbers and various conditions, including stationary and pulsating impinging surfaces. Selimefendigil and Öztop [22] conducted a numerical study on nanofluids involving pulsating rectangular jets. Various parameters, such as oscillation frequency, Reynolds number, and nanoparticle volume concentration, were numerically investigated to assess their effects on the fluid flow and heat transfer characteristics.

To achieve this objective, the study employs advanced numerical simulations using ANSYS to evaluate the effects of double impinging nanofluid jets on heat transfer and flow characteristics across a defined range of Reynolds numbers. In order to comprehensively analyze the problem, several key variables are taken into account, including the type of fluid, nanoparticle concentrations, jet geometry, and pulsating patterns. The study specifically utilizes aluminum oxide (Al_2O_3) nanofluids with varying volume concentrations of 1%, 2%, 4%, and 5%. This approach allows for the investigation of how varying concentrations of nanoparticles affect heat transfer performance, thereby providing valuable insights into the optimization of operational conditions for double impinging jet systems. In conclusion, the results of this study will contribute to a more comprehensive understanding of jet impingement dynamics and enhance the efficiency of thermal management applications.

Mathematical Model and Numerical Method

The reliability of turbulence models is contingent upon the utilization of adequately small mesh elements. Nevertheless, the use of excessively small elements can result in a notable increase in solution times. It is therefore imperative to select an appropriate element size. To investigate this, a mesh independence study was conducted. In the simulations, meshes comprising 200,000, 220,000, and 240,000 nodes were utilized. The resulting solutions facilitated the extraction of Nusselt numbers, and values from three of these meshes were employed to extrapolate the results as if an infinite number of nodes were available. This approach indicated that the results obtained from the mesh with 220,000 nodes reached an accuracy of 0.5%. To guarantee the dependability of the findings, it was imperative that all residuals be reduced to 10^{-8} or below by the conclusion of the computational run. Figure 1 depicts the comprehensive mesh structure, encompassing the number of nodes subjected to testing and a detailed representation of the mesh configuration.

To accurately simulate turbulent flow fields, this study proposes the numerical solution of the two-dimensional turbulent Navier-Stokes and energy equations using a finite-difference scheme, complemented by the continuity equation.

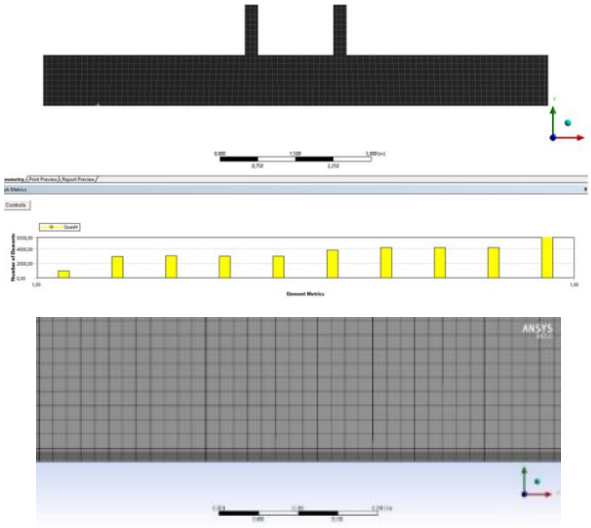

Figure 1. Mesh structure of model.

This approach employs an eddy viscosity model to capture the effects of turbulence under the assumption that the flow is steady, incompressible, and two-dimensional. Furthermore, this analysis excludes the effects of buoyancy and radiation heat transfer, thereby further simplifying the model. The governing equations for mass, momentum, turbulent kinetic energy, turbulent dissipation rate, and energy in a steady turbulent flow are formulated based on the standard κ-ε model, as described in detail below [23];

The momentum, continuity and energy equations, along with the equations of the turbulence model treated as constitutive equations, are presented in the following section [12], [13], [24].

Continuity equation

$$\frac{\partial U_i}{\partial x_i} = 0 \tag{1}$$

The momentum equations, which are the applied form of Newton's Second Law of Motion to fluids, or commonly known as the Navier-Stokes equations applicable for viscous incompressible fluids, are provided below.

$$\rho U_i \frac{\partial U_j}{\partial x_i} = -\frac{\partial P}{\partial x_j} + \frac{\partial}{\partial x_i}\left[\mu\left(\frac{\partial U_i}{\partial x_j} + \frac{\partial U_j}{\partial x_i}\right) - \rho\overline{u_i' u_j'}\right] \tag{2}$$

Energy equation

$$\rho c_p U_i \frac{\partial T}{\partial x_i} = \frac{\partial}{\partial x_i}\left[k\,\frac{\partial T}{\partial x_j} - \rho c_p \overline{u_i' T'}\right] \tag{3}$$

For the κ-ε model, in an incompressible flow, the turbulent kinetic energy κ and the dissipation rate ε are provided respectively [23].

$$\rho U_i \frac{\partial k}{\partial x_i} = \frac{\partial}{\partial x_i}\left[\left(\mu + \frac{\mu_t}{\sigma_k}\right)\frac{\partial k}{\partial x_i}\right] + \mu_t\left(\frac{\partial U_i}{\partial x_j} + \frac{\partial U_j}{\partial x_i}\right)\frac{\partial U_i}{\partial x_j} - \rho\varepsilon \tag{4}$$

$$\rho U_i \frac{\partial \varepsilon}{\partial x_i} = \frac{\partial}{\partial x_i}\left[\left(\mu + \frac{\mu_t}{\sigma_\varepsilon}\right)\frac{\partial \varepsilon}{\partial x_i}\right] + f_1 C_1 \mu_t \frac{\varepsilon}{k}\left(\frac{\partial U_i}{\partial x_j} + \frac{\partial U_j}{\partial x_i}\right)\frac{\partial U_i}{\partial x_j} - f_2 C_2 \rho \frac{\varepsilon^2}{k} \quad (5)$$

In these equations, C_μ, C_1 ve C_2 are empirical constants, while σ_k ve σ_ε are the turbulent Prandtl numbers for the κ ve ε equations, respectively. The symbol μ_t denotes the dynamic viscosity of the fluid. The values of these constants within the turbulence model are specified in equations 4 and 5.

$$\sigma_k = 1, \sigma_\varepsilon = 1{,}314, C_1 = 1.44, C_2 = 1.92, c_\mu = 0.09, c_d = 0.1643 \quad (6)$$

These equations represent mathematical models that elucidate the behavior of fluids and mathematically model turbulence effects. The continuity equation expresses the conservation of mass for the fluid, while the momentum equations describe the fluid's motion. The energy equation is used to calculate the energy transformations of the fluid.

In contrast, turbulence model equations are supplementary equations utilized to quantify turbulence effects, with variations contingent upon the specific turbulence model in question.

The Reynolds number is calculated as follows:

$$Re = \frac{u\, D_h}{v} \quad (7)$$

Here u represents the jet inlet velocity, D_h hydraulic diameter of the jet, v represents the kinematic viscosity.

The Nusselt number and local Nusselt number are determined using the following equations.

$$h = \frac{q}{T_w - T_j} \quad (8)$$

$$Nu = \frac{hD_h}{k} \quad (9)$$

Therefore;

$$Nu = \frac{q\, D_h}{k\,(T_w - T_j)} \quad (10)$$

In the equation, h represents the heat transfer coefficient, q denotes the constant heat flux, k is the thermal conductivity of the fluid, T_w represents the local temperature of the jet surface, and T_j denotes the temperature at the jet exit.

Determination of Boundary Conditions

Figure 2 illustrates the boundary conditions applied to the defined two-dimensional geometry. Within this framework, a custom function has been implemented in the ANSYS software to model the jet velocity, incorporating both a uniform velocity profile and sinusoidal pulsation. Specifically, the jet inlet temperature is set at 298 K, while the impingement surface is maintained at a constant temperature of 400 K. The exit of the jet is exposed to the surrounding environment, thereby applying a free-stream condition.

All other surfaces within the model are treated as adiabatic, indicating that no heat transfer occurs across these boundaries. This assumption streamlines the analysis by negating the loss or gain of heat through the walls. Moreover, the turbulence intensity at the inlet is set at 1%, which facilitates the precise representation of the initial conditions of the jet flow and its interaction with the impinging surface. It is imperative that these boundary conditions are met in order to guarantee the veracity of the numerical simulations and to ensure the reliability of the results obtained from the study of jet impingement behavior.

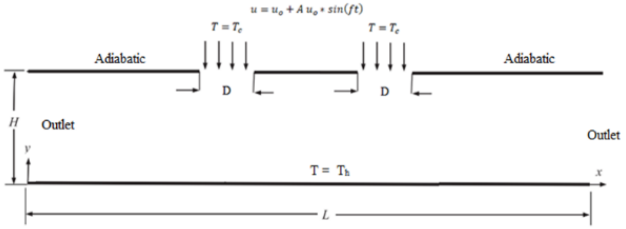

Figure 1. Boundary conditions

These conditions,

$$u = u_o + A\,u_o * sin(ft) \quad (11)$$

$$T = T_c \quad (12)$$

The boundary conditions are employed for the purpose of establishing the velocity and temperature conditions at the jet inlet. The velocity equations demonstrate how the inlet velocity varies over time in relation to a specific function, while the temperature is assumed to remain constant, denoted as T_c. Adiabatic no-slip wall boundary conditions are applied to the upper walls.

$$u = 0, \quad v = 0, \quad \frac{\partial T}{\partial x} = 0 \quad (13)$$

It is crucial to acknowledge that the adiabatic no-slip wall boundary condition is implemented on the upper walls, signifying that heat transfer is not occurring at these surfaces and that the velocity gradient at the wall surface is zero. This boundary condition permits the transfer of momentum while preventing the transfer of thermal energy. Consequently, the velocity components at the wall surface are zero in the direction parallel to the wall, which results in no heat exchange. Such boundary conditions are frequently employed in the context of high-speed flows and scenarios where energy transfer is deemed to be insignificant. In accordance with these adiabatic conditions, no energy is exchanged at the upper wall, thereby influencing solely the momentum of the flow. This is a crucial point for understanding the behavior and interaction of the jet with the upper wall.

The boundary condition for the impinging surface of the jet is as follows;

$$u = 0, \; v = 0, \; T = T_h \quad (14)$$

The boundary conditions applied at the impinging surface of the jet are defined for the velocity components (u and v) and temperature (T). According to this boundary condition, the

velocity components at the impinging surface are assumed to be zero (u = 0, v = 0), indicating no-slip conditions. Furthermore, the temperature of the impinging surface is denoted as T_h. signifying that the surface is maintained at a constant temperature. This boundary condition ensures that the flow velocity is zero at the impinging surface, thereby establishing a stationary interaction between the fluid and the surface.

The boundary condition for the side surfaces of the geometry is as follows;

$$\frac{\partial u}{\partial x} = 0, \qquad \frac{\partial v}{\partial x} = 0, \qquad \frac{\partial T}{\partial x} = 0 \tag{15}$$

The aforementioned boundary conditions indicate that the flow and temperature along the side surfaces of the geometry remain constant in a specific direction, thereby suggesting that the side surfaces are open to the surrounding environment.

Following the model validation, an additional critical step was undertaken: the validation of the numerical study against existing literature. To this end, the accuracy of the numerical study was confirmed by replicating the parameters and features of the previous work conducted by Zumbrumen et al. [25].

The results presented in Figure 3, which illustrate the variation of local Nusselt numbers across the average plate, demonstrate a high degree of consistency. It is noteworthy that a maximum discrepancy of 7% was observed between the local Nusselt numbers reported in the referenced study and those obtained from the current validation model. In conclusion, the findings demonstrate that ANSYS-FLUENT is an effective tool for conducting the numerical analyses planned for the subsequent phases of this research.

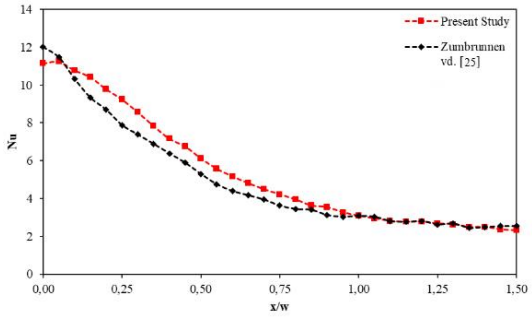

Figure 2. Comparison of numerical study with literature [25].

Results and Discussion

Figure 4 illustrates the time-dependent velocity contours for a pulsating jet with a height-to-diameter ratio (*H/D*) of 4, a Reynolds number (*Re*) of 7500, a frequency (*f*) of 20 Hz, and an amplitude (*A*) of 0.5 m/s. As the jet interacts with the surface, it immediately generates bidirectional swirling flows and reverse vortices in the stagnation region. The vortices undergo a process of evolution over time, exhibiting a trajectory that is parallel to the surface in the direction of flow. The formation of these vortices has the effect of enhancing the coefficients of heat transfer and increasing the Nusselt numbers.

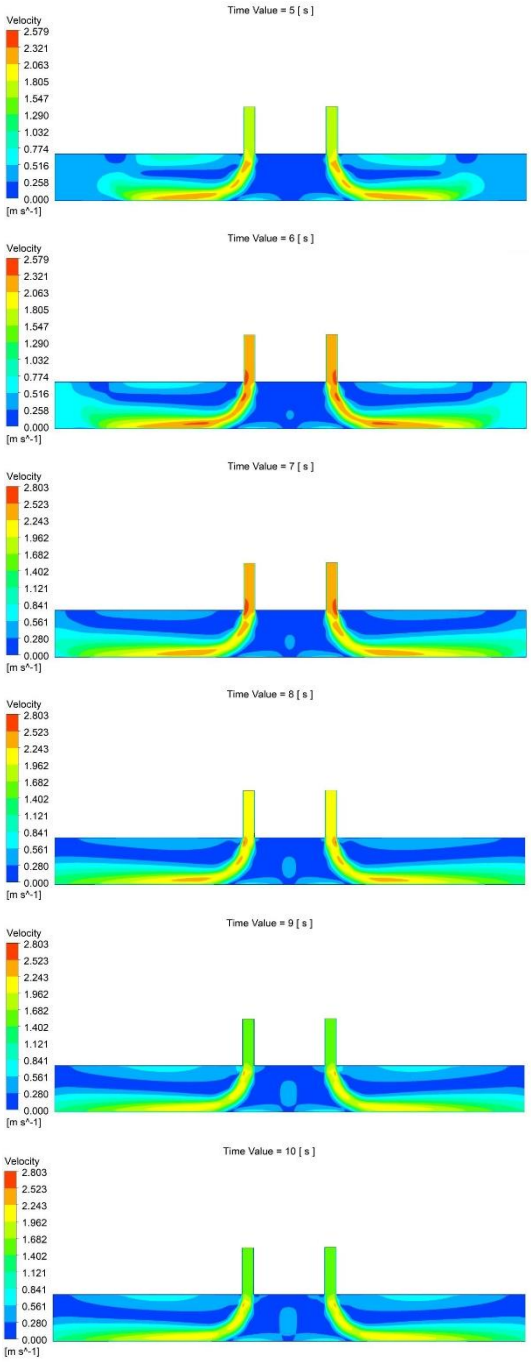

Figure 4. Time-dependent velocity contours of a dual impinging nanofluid jet with *H/D* = 4, *Re* = 7500 for *t* = 5 - 10 sn.

At the point of jet exit, the flow profile is initially uniform. However, as the jet ascends vertically, there is a notable change in the velocity distribution. The maximum velocity is observed along the axis of the jet, but upon contact with the lower plate, the velocity decreases to zero. Subsequently, the flow undergoes horizontal acceleration along the surface, resulting in the formation of a wall jet. Upon contact with the surface, the jet decelerates to zero, resulting in the formation of an internal vortex. This process ultimately results in the formation of a smaller vortex in close proximity to the target surface, accompanied by the emergence of another vortex in a downstream position.

It is noteworthy that the jet velocity does not reach zero throughout the entire flow period, which accounts for the limited formation of small vortices near the adiabatic wall and heated surface [26]. With regard to Reynolds numbers, a typical impinging jet exhibits characteristics analogous to those of a free jet, including a stagnation or impingement zone and a wall jet region.

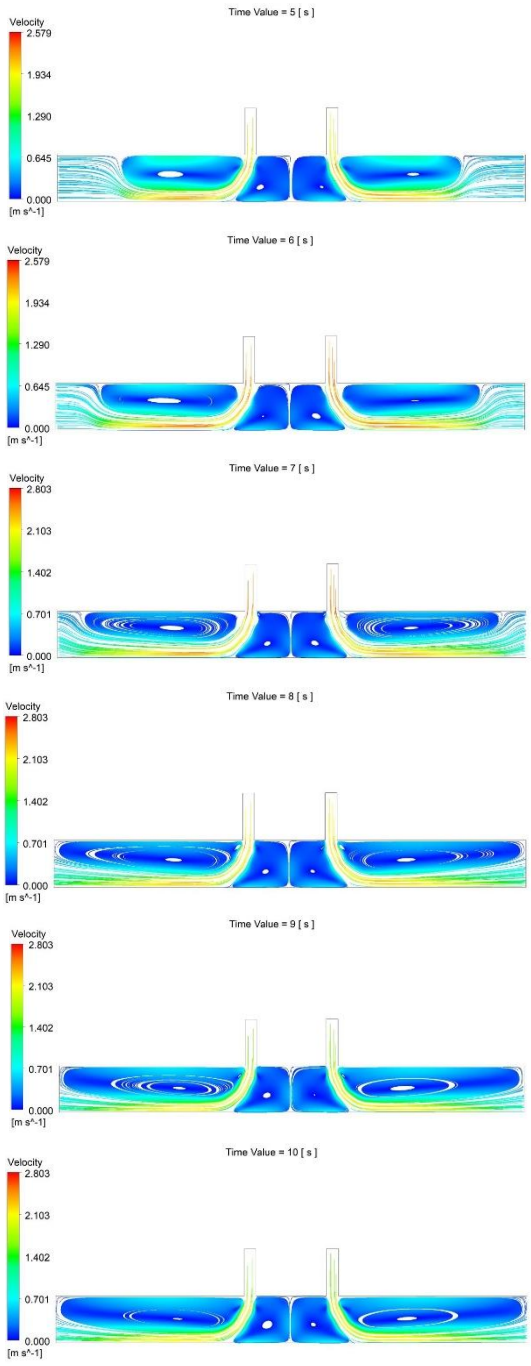

Figure 5. Time-dependent streamlines of a dual impinging nanofluid jet with a *H/D* = 4, *Re* = 7,500 for *t* = 5 - 10 sn.

Figure 5 illustrates the time-dependent streamlines of a dual jet configuration. It becomes evident that the velocity within the wall jet region increases upon impact with the impinging surface over time. Initially, the impinged surface maintains a constant temperature of 400 degrees Celsius. Upon impact, the jets induce a cooling effect on the impinging surface. As the two jets make contact with the surface, the distance between them widens, indicating a divergence upon impact. Moreover, in the analyzed configuration, the adjacent jets remain independent of one another until they reach the impinging surface, resulting in the formation of separate vortices within each jet. Furthermore, the impinging surface causes the thermal boundary layer to experience peak velocities in its upper section, resulting in the formation of additional vortices. At the initial time point of t = 5 seconds, the vortices are relatively small in size. However, as time progresses, there is an observable increase in the size of these vortices. At the point of jet exit, the velocity reverts to a uniform profile.

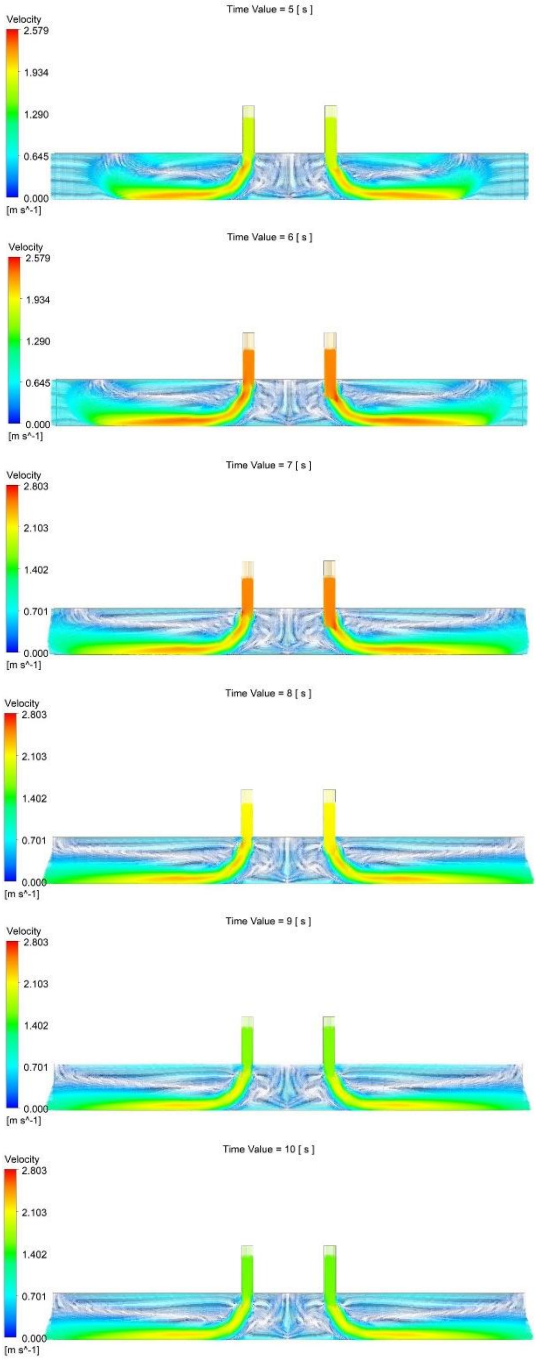

Figure 6. Time-dependent vector representation of a dual impinging nanofluid jet with a *H/D* = 4, *Re* = 7,500 for *t* = 5 - 10 sn.

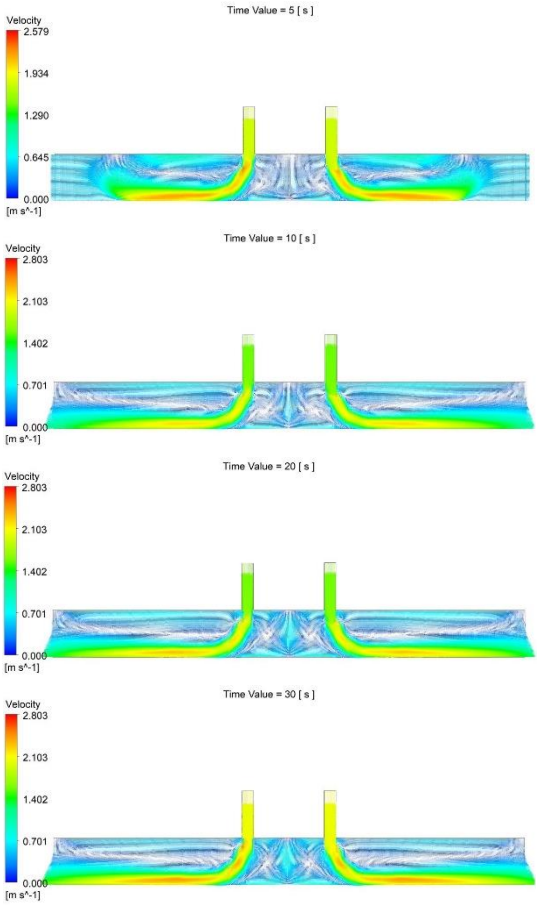

Figure 7. Time-dependent vector representation of a dual impinging nanofluid jet with a *H/D* = 4, *Re* = 7,500 for *t* = 5 - 30 sn.

Figures 6 and 7 illustrate the time-dependent vector fields for a dual pulsating jet with a height-to-diameter ratio (*H/D*) of 4, a Reynolds number (*Re*) of 7,500, a frequency (*f*) of 30 Hz, and an amplitude (*A*) of 0.4 m/s. Upon impacting the heated lower surface, the formation of two counter-rotating vortices becomes evident, resulting from confinement by the upper adiabatic plate and the inherent sensitivity of the jet. A symmetrical flow pattern is observed in both the flow and thermal fields, centered around the stagnation point.

While slight variations are discernible in the vector plots across different time intervals, the intensity of the vortices exhibits fluctuations. In the wall jet region, an increase in thickness is observed concomitant with a decrease in the normal component of velocity. Moreover, as the volume concentration of nanoparticles increases, the effective thermal conductivity of the nanofluid rises, resulting in enhanced cooling effects upon impingement and a more uniform temperature distribution, thereby improving heat transfer. Moreover, the frequency and amplitude of pulsating in the inlet velocity contribute to a denser arrangement of flow lines in this region, which significantly enhances heat transfer [27].

Figure 8. shows the local Nusselt number variation as a function of 's', the distance between the two jets in a dual-jet setup. The study investigates how the distance between jets affects the change in Nusselt number, with experiments conducted for *H/D* = 4 and *Re* = 10,000. The findings demonstrate a direct correlation between the distance between the jets and the efficiency of heat transfer. A closer proximity between the jets facilitates enhanced interaction through vortex formation, which has a beneficial impact on the Nusselt number. Conversely, an increase in the distance between the jets has been observed to result in a decline in the Nusselt number.. As shown in Figure 8, the optimal local Nusselt number is achieved when 's' is set at 100 mm, indicating superior heat transfer performance compared to other distances.

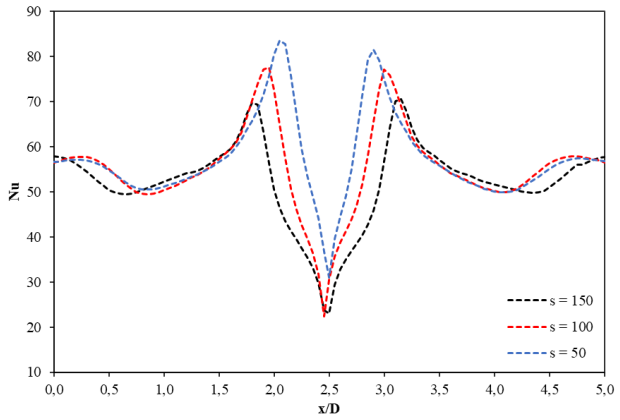

Figure 8. Comparison of distances between dual impinging jets.

Figure 9 shows the variation of local Nusselt numbers for different nanoparticle volume concentrations for *Re* = 5000, *f* = 20 Hz, and *A* = 0.5 m/s. In the case of dual impinging jets, the collision generates two distinct peaks in the Nusselt number profile. The highest Nusselt value is observed at the stagnation point, where the thermal boundary layer is relatively thin, resulting in enhanced heat transfer. The incorporation of nanoparticles at varying concentrations markedly enhances the peak Nusselt value, suggesting an acceleration in heat transfer rates. Moreover, an increase in the volume concentration of nanoparticles results in a more pronounced improvement in heat transfer. In comparison to the scenario in the absence of nanoparticles, the Nusselt number demonstrates an 18% increase at a 5% volume concentration, a 16% increase at both 4% and 2% concentrations, and a 13% increase at a 1% concentration.

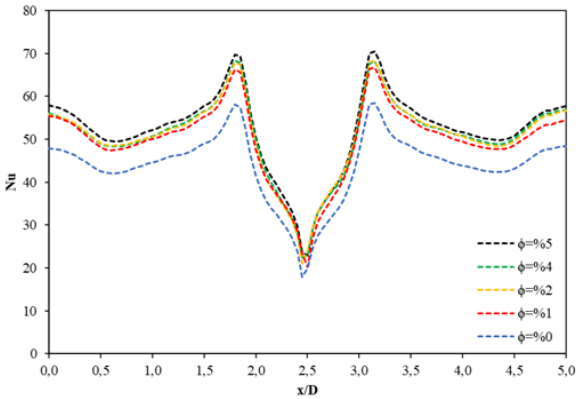

Figure 9. Local Nusselt number variation for different nanoparticle volume concentrations for *H/D* = 4 and *Re* = 5,000.

Figure 10 illustrates the impact of varying frequencies on the local Nusselt numbers for a dual impinging jet, with a Reynolds number of 7500 and an acceleration coefficient of 0.5 m/s. The occurrence of pulsating flow results in acceleration and elevated speeds, which contribute to augmented heat transfer due to the fact that a fluid with greater velocity carries more energy and interacts with the surface in a more efficacious manner. Pulsating flow has the potential to alter the temperature distribution by facilitating a more rapid and intense mixing between regions of differing temperatures, thereby promoting a more uniform temperature profile. These dynamics are of critical importance in the observed enhancement of heat transfer in pulsating flows. Pulsations facilitate more efficient mixing, enhance energy transport through accelerated fluid movement, and influence temperature distribution, ultimately leading to heightened heat transfer rates. It can be concluded that pulsating flow has a considerable effect on thermophysical performance and heat transfer efficiency [28], [29]. The data analysis indicates that the most substantial enhancement in heat transfer on the impinging surface occurs at a frequency of 30 Hz. A comparison of frequencies at 10 Hz and 30 Hz indicates a 10% increase in heat transfer efficiency. It can thus be concluded that pulsating jets with higher frequencies enhance heat transfer performance in the wall jet region, resulting in a more uniform heat distribution on the target surface, particularly in the vicinity of the stagnation point [26].

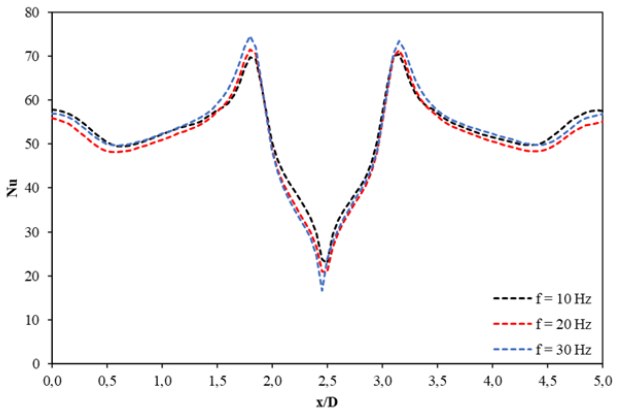

Figure 10. Local Nusselt number variation for different frequencies in a dual impinging jet with *Re* = 7500 and amplitude *A* = 0.5 m/s.

Figure 11 illustrates the variation in local Nusselt numbers for different amplitudes, with *Re* = 7500 and *f* = 20 Hz. While the results for all amplitudes are relatively similar, the amplitude of 0.5 m/s exhibits superior performance due to its wider distribution across the impinging surface. The pulsating flow enhances mixing, increases energy transport through accelerated fluid movement, and modulates temperature distribution, resulting in improved heat transfer rates. Therefore, pulsating flow significantly impacts thermophysical performance and heat transfer efficiency [28], [29].

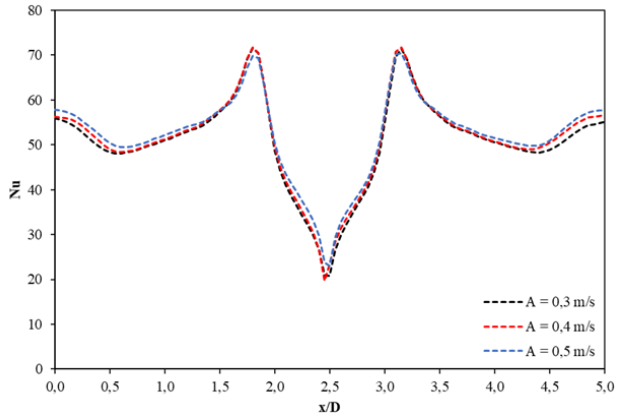

Figure 11. Local Nusselt number variation for different amplitudes in a dual impinging jet with *Re* = 7500 and frequency *f* = 20 Hz.

Conclusion

In this study, the flow dynamics and heat transfer interaction in double-pulsed jets are investigated, focusing on key factors such as jet geometry, vibration frequency, amplitude, nanoparticle concentration and Reynolds numbers. Using advanced numerical simulations in ANSYS, the research investigates how these parameters affect the thermal and flow properties of pulsating nanofluid jets.

This study systematically analyses the impact of diverse factors on the performance and characteristics of double impinging jets, with a particular focus on the crucial interplay between flow dynamics and heat transfer efficiency. The research employs advanced numerical simulations with ANSYS to assess the influence of double impinging nanofluid jets across a defined range of Reynolds numbers. This comprehensive analysis encompasses a multitude of parameters, including jet geometry, pulsating frequency and amplitude, nanoparticle volume concentrations, and Reynolds numbers.

The time-dependent velocity contours of the pulsating jet demonstrate that as the jet makes contact with the surface, bidirectional swirling flows and reverse vortices are produced. These vortices expand and follow parallel paths along the flow direction, resulting in an increased heat transfer coefficient and elevated Nusselt number. The formation of wall jets is observed as the flow transitions from its initial smooth profile at the jet's exit. While the highest velocity is observed at the jet's axis, the impact with the surface results in deceleration and the formation of internal vortices, which contribute to the development of horizontal wall jets along the surface.

The frequency and amplitude of pulsating jets significantly influence heat transfer efficiency. Higher frequencies, such as 30 Hz, have been observed to result in a 10% improvement in heat transfer compared to lower frequencies like 10 Hz. This enhancement is attributed to improved flow dynamics and more uniform heat distribution facilitated by pulsation and the generation of associated vortices. Additionally, the concentration of nanoparticles plays a crucial role in heat transfer performance. For instance, a 5% volume concentration of nanoparticles led to an 18% increase in the Nusselt number compared to cases without nanoparticles,

highlighting the potential of nanoparticle augmentation to enhance heat transfer efficiency.

It would be beneficial to gain an understanding of the characteristics of the thermal boundary layer in order to elucidate the relationship between Reynolds numbers and heat transfer. It seems that an increase in Reynolds number may result in a reduction in the thickness of the boundary layer, thereby enhancing the rate of heat transfer.

It has been observed that the stagnation point exhibits peak Nusselt values due to the thin boundary layer, whereas regions devoid of vortices display lower Nusselt values. The spacing between dual impinging jets is identified as a critical parameter influencing heat transfer performance. Smaller distances between jets enhance vortex interactions, promoting more effective heat transfer, while larger separations weaken these interactions and reduce overall efficiency. This study establishes that an optimal spacing of approximately 100 mm yields the best heat transfer results, underscoring the importance of jet configuration in optimizing heat distribution and thermal efficiency. Moreover, the findings emphasize the need to optimize key parameters, including frequency, amplitude, nanoparticle volume concentration, and jet spacing, to significantly improve heat transfer and thermophysical performance across various applications.

References

[1] Y. J. Chou and Y. H. Hung, "Impingement cooling of an isothermally heated surface with a confined slot jet," *J. Heat Transfer*, vol. 116, no. 2, pp. 479–482, May 1994, doi: 10.1115/1.2911422.

[2] A. H. Beitelmal, M. A. Saad, and C. D. Patel, "The effect of inclination on the heat transfer between a flat surface and an impinging two-dimensional air jet," *Int. J. Heat Fluid Flow*, vol. 21, no. 2, pp. 156–163, Apr. 2000, doi: 10.1016/S0142-727X(99)00080-6.

[3] Y. M. Chung, K. H. Luo, and N. D. Sandham, "Numerical study of momentum and heat transfer in unsteady impinging jets," *Int. J. Heat Fluid Flow*, vol. 23, no. 5, pp. 592–600, Oct. 2002, doi: 10.1016/S0142-727X(02)00155-8.

[4] B. Sagot, G. Antonini, A. Christgen, and F. Buron, "Jet impingement heat transfer on a flat plate at a constant wall temperature," *Int. J. Therm. Sci.*, vol. 47, no. 12, pp. 1610–1619, 2008, doi: https://doi.org/10.1016/j.ijthermalsci.2007.10.020.

[5] Z. Trávníček, P. Dančová, J. Kordík, T. Vít, and M. Pavelka, "Heat and mass transfer caused by a laminar channel flow equipped with a synthetic jet array," *J. Therm. Sci. Eng. Appl.*, vol. 2, no. 4, Feb. 2011, doi: 10.1115/1.4003428.

[6] F. Afroz and M. A. R. Sharif, "Numerical study of heat transfer from an isothermally heated flat surface due to turbulent twin oblique confined slot-jet impingement," *Int. J. Therm. Sci.*, vol. 74, pp. 1–13, 2013, doi: https://doi.org/10.1016/j.ijthermalsci.2013.07.004.

[7] T. Demircan and H. Turkoglu, "Numerical analysis of effects of the oscillation characteristics and the nozzle to plate distance on the flow and heat transfer in oscillating impinging jets," *Cilt*, vol. 25, no. 4, pp. 895–904, 2010.

[8] N. Çelik, "Investigation of the effects of optimum nozzle type on the impinging jest", Ph.D. dissertation, Dept. Mech. Eng., Firat Univ., Elazığ, TR, 2006.

[9] N. Çelik, D.W. Bettenhausen, D. Ryan Lovik, "Formation of Co-Axıal jets and their downstream development", 2012.

[10] N. Çelik, H. Eren, "Effects of stagnation region turbulence of an impinging jet on heat transfer", J. Therm. Sci. Technol., vol. 30, pp. 91–98, 2010.

[11] A. Nabadavis, D.P. Mishra, "Numerical investigation of jet impingement heat transfer on a flat plate, Carbon - Sci. Technol., vol. 8, pp. 1–12, 2016.

[12] J. Y. San and J. J. Chen, "Effects of jet-to-jet spacing and jet height on heat transfer characteristics of an impinging jet array," *Int. J. Heat Mass Transf.*, vol. 71, pp. 8–17, 2014, doi: 10.1016/j.ijheatmasstransfer.2013.11.079.

[13] S. S. N. Chougule N.K., Parishwad G.V., Gore P.R., Pagnis S., "CFD Analysis of multi-jet air impingement on flat plate," 2011.

[14] S. Caliskan, S. Baskaya, and T. Calisir, "Experimental and numerical investigation of geometry effects on multiple impinging air jets," *Int. J. Heat Mass Transf.*, vol. 75, pp. 685–703, 2014, doi: 10.1016/j.ijheatmasstransfer.2014.04.005.

[15] M. A. Pakhomov and V. I. Terekhov, "Numerical study of fluid flow and heat transfer characteristics in an intermittent turbulent impinging round jet," *Int. J. Therm. Sci.*, vol. 87, pp. 85–93, 2015, doi: https://doi.org/10.1016/j.ijthermalsci.2014.08.007.

[16] E. C. Mladin and D. A. Zumbrunnen, "Local convective heat transfer to submerged pulsating jets," *Int. J. Heat Mass Transf.*, vol. 40, no. 14, pp. 3305–3321, 1997, doi: 10.1016/S0017-9310(96)00380-8.

[17] D. J. Sailor, D. J. Rohli, and Q. Fu, "Effect of variable duty cycle flow pulsations on heat transfer enhancement for an impinging air jet," *Int. J. Heat Fluid Flow*, vol. 20, no. 6, pp. 574–580, 1999, doi: 10.1016/S0142-727X(99)00055-7.

[18] R. Zulkifli, K. Sopian, S. Abdullah, and M. Takriff, "Comparison of local nusselt number between steady and pulsating jet at different jet reynolds number," 2009.

[19] T. S. Zhao and P. Cheng, "Oscillatory heat transfer in a pipe subjected to a laminar reciprocating flow," *J. Heat Transfer*, vol. 118, no. 3, pp. 592–597, Aug. 1996, doi: 10.1115/1.2822673.

[20] T. Demircan and H. Turkoglu, "The numerical analysis of oscillating rectangular impinging jets," *Numer. Heat Transf. Part A Appl.*, vol. 58, no. 2, pp. 146–161, 2010, doi: 10.1080/10407782.2010.496669.

[21] Chaugule, V., Narayanaswamy, R., Lucey, A.D., Narayanan, V., Jewkes, J. (2018). Particle image velocimetry and infrared thermography of turbulent jet impingement on an oscillating surface. Experimental Thermal and Fluid Science. 98, 576–593.

[22] Selimefendigil, F., Öztop, H.F. (2014). Pulsating nanofluids jet impingement cooling of a heated horizontal surface. International Journal of Heat and Mass Transfer. 69 54–65.

[23] E. M. Alawadhi, "Meshing guide," *Finite elem. simulations using ANSYS*, vol. 15317, no. November, pp. 407–424, 2020, doi: 10.1201/b18949-12.

[24] "Fluent12," *ANSYS FLUENT 12.0 User's Guid.*, no. April, pp. 1–2070, 2009.

[25] D. A. Zumbrunnen, F. P. Incropera, and R. Viskanta, "A laminar boundary layer model of heat transfer due to a nonuniform planar jet impinging on a moving plate," *Wärme- und Stoffübertragung*, vol. 27, no. 5, pp. 311–319, 1992, doi: 10.1007/BF01589969.

[26] P. Li, D. Guo, and R. Liu, "Mechanism analysis of heat transfer and flow structure of periodic pulsating nanofluids slot-jet impingement with different waveforms," *Appl. Therm. Eng.*, vol. 152, pp. 937–945, Apr. 2019, doi: 10.1016/j.applthermaleng.2019.01.086.

[27] G. A. Rao, M. Kitron-Belinkov, and Y. Levy, "Numerical analysis of a multiple jet impingement system," *Proc. ASME Turbo Expo*, vol. 3, no. PART A, pp. 629–639, 2009, doi: 10.1115/GT2009-59719.

[28] N. C. Roy, "Steady and Oscillating Characteristics of Natural Convection in an Enclosure," *J. Thermophys. Heat Transf.*, vol. 35, no. 2, pp. 268–278, Oct. 2020, doi: 10.2514/1.T6117.

[29] W. Liewkongsataporn, T. Patterson, and F. Ahrens, "Pulsating jet impingement heat transfer enhancement," *Dry. Technol.*, vol. 26, no. 4, pp. 433–442, 2008, doi: 10.1080/07373930801929268.